ChemComm

Chemical Communications

Accepted Manuscript

This article can be cited before page numbers have been issued, to do this please use: J. Zhang, Z. Tan, W. LENG , Y. Chen, S. Zhang, B. T. W. Lo, K. K. Yung and Y. Peng, *Chem. Commun.*, 2020, DOI: 10.1039/D0CC02351E.

View Article Online
DOI: 10.1039/D0CC02351E

COMMUNICATION

Chemical State Tuning of Surface Ce Species on Pristine CeO_2 with 2400% Boosting in Peroxidase-like Activity for Glucose Detection

Received 00th January 20xx,
Accepted 00th January 20xx

DOI: 10.1039/x0xx00000x

Jieru Zhang, [a] Zicong Tan, [a] Wanying Leng, [a] Yu-Cheng Chen, [b] Shiqing Zhang, [c] Benedict T.W. Lo, [d] Ken Kin Lam Yung [c] and Yung-Kang Peng*[a,e]

We demonstrate that the Ce reactivity of CeO_2 towards H_2O_2 is dictated by its local structure and electron density. More than 2400% increase in peroxidase-like activity has been achieved on the (100) surface for glucose detection due to the promoted H_2O_2 adsorption and subsequent activation by the electron-rich Ce species.

Nowadays, commercial glucose detection kits for clinical or laboratory use are based on a well-established "enzymatic assay" which involves two consecutive enzyme reactions. As shown in **Scheme 1a**, the oxidation of glucose by the glucose oxidase to produce H_2O_2 (from the reduction of oxygen, reaction I), which in the second step, is reduced by horseradish peroxidase (HRP) with the oxidation of dye to generate a colour change (reaction II). The colour change thus reflects glucose in blood/solution, and its concentration can be obtained by the intensity at a specific wavelength. Despite the wide use of this commercial assay, the intrinsic drawback of natural enzyme is the easy denaturation and high costs in both preparation and purification. The use of natural enzymes in both portable monitor and laboratory research kit has made their price widely unaffordable. The progress of relevant research is thus severely slowed down in the past decades.

Extensive efforts have been devoted to developing enzymes' alternatives called "artificial enzymes", which possess advantages such as low-cost in mass production, simple storage, recyclability and pH/thermal stability. Among various artificial enzymes, nanomaterial-based products have received considerable attention over the past few years since the discovery of Fe_3O_4 nanoparticles with peroxidase-like activity.[1] Since then, transition metal-based oxide nanomaterials (e.g. Co_3O_4, Fe_3O_4, CuO and CeO_2), have been reported can mimic peroxidase (a.k.a. nanozymes) due to their switchable oxidation states.[2–4] The peroxidase mimicking activities are often evaluated by the catalytic reaction between H_2O_2 and tetramethylbenzidine (TMB) (i.e. reaction II in **Scheme 1b**). The reduction of H_2O_2 to H_2O firstly catalyses the oxidation of surface cation of nanozyme from M^{n+} to $M^{(n+1)+}$. The $M^{(n+1)+}$ subsequently oxidizes TMB to generate a colour change at 652 nm. The whole cycle can be completed by the regeneration of M^{n+} for the next catalytic cycle. Accordingly, the sensing of H_2O_2 (produced in reaction I) by M^{n+} on the topmost surface of nanozyme is believed the key to obtaining high glucose sensitivity when HRP is replaced in the consecutive enzyme reactions **(Scheme 1b)**.

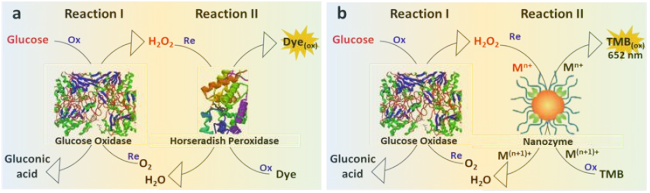

Scheme 1. The working principle of the colorimetric assay for glucose detection: (a) Conventional "enzymatic assay" using Horseradish peroxidase (HRP) as the second enzyme. (b) Using artificial nanozyme to mimic HRP in the second enzymatic reaction of glucose detection (TMB: tetramethylbenzidine).

To achieve this goal, researchers have dedicated in the surface engineering of nanozyme for high $M^{n+}/M^{(n+1)+}$ ratio over the past decade. Taking CeO_2 as an example, H_2O_2 post-treatment on pristine CeO_2 sphere has been adopted to tune surface Ce^{3+}/Ce^{4+} ratio by reducing Ce^{4+} to Ce^{3+}.[5,6] Qu et al. reported another effective method to enhance the surface Ce^{3+}/Ce^{4+} ratio by treating CeO_2 rod hydrothermally with water at 160 °C.[7–9] The Ce^{3+} fraction of the resulting porous CeO_2 rod was found doubled and plays a key role in mimicking not only peroxidase[7] but also phosphatase[8] and photolyase.[9] However, only a little enhancement (< 200%) in the peroxidase-like activity of CeO_2 was achieved after those post-treatments over the past years.[5–11]

Since the oxidation of TMB (i.e. the colour indicator) is initiated by H_2O_2 sensing at the surface of CeO_2 nanozyme, the chemical state of surface Ce can thus affect its peroxidase-like activity. This factor can be fine-tuned on pristine CeO_2 by exposing different facets.[12,13] **Figure 1** shows three surface structures of

[a] *Department of Chemistry, City University of Hong Kong, Hong Kong, China.*
[b] *Department of Mechanical Engineering, City University of Hong Kong, Hong Kong, China.*
[c] *Department of Biology, Hong Kong Baptist University, Hong Kong, China.*
[d] *Department of Applied Biology and Chemical Technology, Hong Kong Polytechnic University, Hong Kong, China.*
[e] *City University of Hong Kong Shenzhen Research Institute, Shenzhen 518057, China.*

Electronic Supplementary Information (ESI) available: Detailed preparation, characterization and catalytic testing of CeO_2 shape. See DOI: 10.1039/x0xx00000x

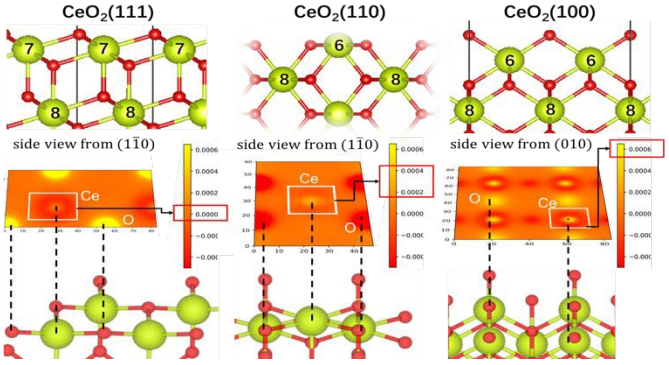

Figure 1. Surface crystallographic CeO_2(111), CeO_2(110) and CeO_2(100) structures. The number labelled on Ce atom shows its coordination number. Middle row: the difference in electron density between saturated Ce in bulk (8 coordination) and surface unsaturated Ce on CeO_2 facets. Noted that the electron density of 7-coordinated Ce on CeO_2(111) was set at 0.0000 for comparison (see SI for details).

most common CeO_2 facets. The atomic arrangement and coordination environment of surface Ce atoms are different on the (111), (110) and (100) facets. The difference in electron density between Ce in bulk (8 coordination; Ce-O) and surface unsaturated Ce was further compared in the bottom row of **Figure 1**. Since the Ce atom with lower coordination number should possess higher electron density, the 6-coordinated Ce on both CeO_2(110) and CeO_2(100) shows higher electron density than the 7-coordinated Ce on CeO_2(111) as expected. However, it is interesting that Ce on CeO_2(100) has higher electron density than its counterpart on CeO_2(110) presumably due to the relaxation of this high-energy facet.[12,13] According to above structural analysis, the electron density of surface Ce atoms is demonstrated to change "continuously" with the atomic arrangement and coordination environment of their host surfaces in the order of (100) > (110) > (111).

To experimentally evaluate the role of Ce electron density in peroxidase mimicking, CeO_2 octahedron, rod and cube majorly terminated (111), (110) and (100) facets were prepared based on methods adopted in literature.[14] The shape and size of the as-prepared CeO_2 samples were characterized by transmission electron microscopy (TEM). **Figure 2a** shows CeO_2 octahedron with a narrow size distribution between 15 and 20 nm. The rod-shaped CeO_2 has a diameter of 10 nm and length up to 200 nm **(Figure 2b)**. A relatively wider size distribution can be observed for CeO_2 cube with lateral length ranging from 20 to 50 nm **(Figure 2c)**. High-resolution TEM (HRTEM) characterization was further carried out on three CeO_2 shapes **(Figure S1)** to confirm the preferential exposure of the targeted facets. Even though the surface of rod seems ill-defined **(Figure S1b)**, we assume herein the majority of rod surface is terminated by the (110) facet as often assigned in literature.[12–14] X-ray powder diffraction (XRD) results of CeO_2 shapes in **Figure S2** confirm their fluorite structure (JCDPS no. 65-2795). According to the surface area measurements **(Table S1)**, rod-shaped CeO_2 possesses the highest surface of 95 m^2/g followed by octahedron (46 m^2/g) and cube (29 m^2/g).

The peroxidase mimicking activity of CeO_2 shapes (i.e. reaction II in **Scheme 1b**) was then evaluated by the formation of TMB_{ox} with a colour change at 652 nm. As shown in **Figure 2d**, cube

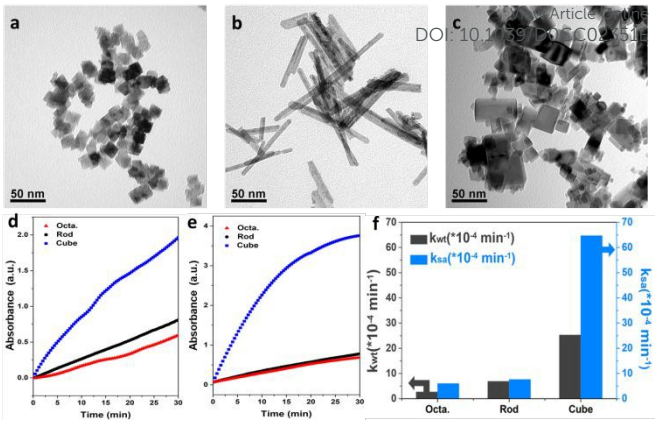

Figure 2. Transmission electron microscope (TEM) images of CeO_2 (a) octahedron, (b) rod and (c) cube. The time-dependent peroxidase mimicking activity over CeO_2 shapes with same tested (d) weight (i.e. 1 mg for each shape), (e) surface area (i.e. 2 mg for for octahedron, 1 mg for rod and 3.3 mg for cube) and (f) corresponding first-order k constants. Note that k_{wt} and k_{sa} represents the k constant of reaction carried out using the same catalyst weight and surface area, respectively.

provides the highest activity among the three shapes followed by rod and octahedron (1 mg of sample was tested). The corresponding first-order rate constant k_{wt} ($\times 10^{-4}$ min^{-1}) was calculated as: 25.3 for cube > 6.9 for rod > 2.7 for octahedron **(Figure 2f and Figure S3a)**. This order matches well with the corresponding electron densities of Ce on CeO_2 facets as predicted above (i.e. (100) > (110) > (111)), suggesting that the reactivity of Ce could significantly vary with the hosted facet. Since CeO_2 shapes possess different surface areas, they were further tested under similar surface area for a better comparison (i.e. 2 mg for octahedron, 1 mg for rod and 3.3 mg for cube). As expected, cube again outperforms the other two shapes **(Figure 2e)** with corresponding k_{sa} constant ($\times 10^{-4}$ min^{-1}) in the order of 64.7 (cube) > 7.6 (rod) > 6.0 (octahedron) **(Figure 2f and Figure S3b)**. The peroxidase-like activity of CeO_2 is thus shape-dependent and can enhance both k_{wt} and k_{sa} constants by about 10 times, when the surface is changed from octahedron (111) to cube (100). This result indicates that both the local structure and electron density of Ce on pristine CeO_2 can lead to a huge difference in their peroxidase-like activity.

However, very similar XPS Ce_{3d} results were obtained for CeO_2 shapes **(Figure 3a)**. We believe this is due to the photoelectrons collected by XPS depending heavily on the electron escaping depth. For example, the penetration depth for Ce_{3d} photoelectrons with 550 eV kinetic energy has been reported to penetrate > 5 nm from CeO_2 surface using commercial XPS instrument.[15] Considering the size of CeO_2 shapes used in this study **(Figure 2a–c)**, XPS Ce_{3d} signals from the topmost Ce atoms (i.e. the active site) were significantly diluted. It thus makes no sense to correlate the XPS results of a nanocrystal with catalytic reactions that only involve active sites on its topmost surface.[16] Some literature even use Ce^{3+}/Ce^{4+} ratio obtained from XPS spectra deconvolution for quantitative correlation.[5–14,17–19] The Ce^{3+}/Ce^{4+} ratio for CeO_2 shapes was then calculated as: 0.15 for octahedron, 0.25 for rod and 0.18 for cube **(Table S1 & Figure S4)**. It is understandable that Ce^{3+} can reduce H_2O_2 to H_2O easier (cf. Ce^{4+}) and hence a higher Ce^{3+}/Ce^{4+} ratio should offer a better peroxidase mimicking activity. However, no such correlation

View Article Online
DOI: 10.1039/D0CC02351E

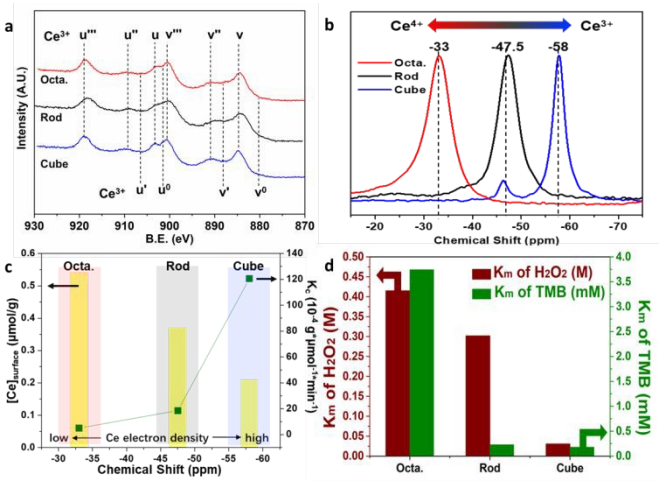

Figure 3. (a) XPS Ce_{3d} and (b) TMP-^{31}P NMR spectra of CeO_2 shapes. (c) Correlation plot of Ce electron density and $[Ce]_{surface}$ of CeO_2 shapes with corresponding kc constant (10^{-4} g*μmol^{-1}*min^{-1}) (i.e. derived from $k_{wt}/[Ce]_{surface}$). (d) Comparison between the K_m of H_2O_2 and TMB obtained by Michaelis-Menten analysis over CeO_2 shapes.

can be observed in **Figure 2f**. More importantly, we cannot explain why the Ce^{3+} portion of cube (15.44%) is very active while it is inactive for octahedron with only 2% less of Ce^{3+} (13.37%). The discussion above on XPS strongly suggests that (1) it is not sensitive to Ce (i.e. the active site) on the topmost surface of CeO_2, and (2) the chemical state of Ce cannot be "discretely" classified into either 3+ or 4+. Unfortunately, most researchers have failed to acknowledge both points during their catalytic correlations, leading to different interpretations found over the past decades.[5–14,17–19] Even though some literature have employed Raman and infrared (IR) in combination with surface probes such as MeOH,[20] pyridine/CD_3CN[21] and CO[22] to study the topmost surface of CeO_2 shapes. Unfortunately, none of above molecules can reveal the facet-electron density relationship suggested above (i.e. (100) > (110) > (111)) since they are too basic to distinguish Ce atoms among CeO_2 facets by the given technique.[23]

Phosphorus-containing molecule such as trimethylphosphine (TMP) has been demonstrated a sensitive ^{31}P NMR probe for acidic study on various zeolite-derivatives since 1984.[23–27] The coordination of TMP to a surface cation (i.e. Ce here) will generate ^{31}P signal with a chemical shift (δ^{31}P) between −20 to −61 ppm depending on its acidity (or electron density). A more acidic surface Ce interacts more strongly with the lone pair electron of TMP and hence downshift the δ^{31}P, resulting in a more positive shift. The TMP-^{31}P NMR spectra of CeO_2 shapes in **Figure 3b** clearly show that the electron density of surface Ce is shape-dependent with decreased ^{31}P shielding from −58 ppm (cube), −47.5 ppm (rod) to −33 ppm (octahedron). This order matches perfectly the predicted electron density in **Figure 1**, confirming the surface Ce has the highest electron density on (100) facet while lowest on (111) facet.[27] This facet-dependent electron density of surface Ce was visualized recently by a STEM-EELS study that 3+-like Ce was found on (100) surface while 4+-like Ce on that of (111) surface.[28] Most importantly, the descriptor (i.e. δ^{31}P) can reveal the continuous change of Ce electron density resulting from different atomic arrangements and coordination environments among CeO_2 surfaces **(Figure 1)**.

Thanks to the quantitative nature of NMR, the concentration of surface Ce ($[Ce]_{surface}$) was obtained by the amount of surface adsorbed TMP **(Table S1)**. Interestingly, the sample with a high surface area does not guarantee high concentration of active sites. Since $[Ce]_{surface}$ **(Table S1)** shows an inverse trend to both k_{wt} and k_{sa} **(Figure 2f)**, the $[Ce]_{surface}$ is thus not the key factor affecting the observed mimicking activity among CeO_2 shapes. Instead, all evidences suggest that the surface Ce with higher electron density can facilitate H_2O_2 reduction and hence accelerate the reaction II in **Scheme 1b**. To study the electron density-reactivity correlation of surface Ce, the k_{wt} was further normalized by $[Ce]_{surface}$ (denoted as k_c) in **Figure 3c**. The k_c constant (10^{-4} g·μmol^{-1}·min^{-1}), which represents the specific reactivity of surface Ce, was then calculated as 5 for octahedron, 18.6 for rod and 120.5 for cube. It is surprising that 370% and 2400% increase in corresponding k_c can be achieved when the electron density of Ce is tuned by simply changing its host surface from (111) to (110) and (100).

Michaelis–Menten analysis on CeO_2 shapes was then carried out to study the affinity of reactant molecules (i.e. H_2O_2 **(Figure S5a)** and TMB **(Figure S5b)**) as a function of their concentration. A series of Michaelis constants (K_m) and maximum initial reaction rates (V_{max}) were summarized in **Table S2**. In general, a higher K_m value indicates a lower affinity of substrate to catalyst, hence a lower mimicking activity.[2–4] As expected, H_2O_2 and TMB both exhibit the lowest affinity to CeO_2 octahedron followed by rod and cube with decreasing K_m value **(Figure 3d)**. Even though the rod shows comparable TMB K_m with the cube, its low peroxidase-like activity **(Figure 2f)** can be attributed to the low H_2O_2 affinity of rod surface (same as the octahedron). This result thus suggests that the sensing of H_2O_2 by CeO_2 surface is the key step (cf. TMB) dictating its mimicking activity. Similar explanation can be extended to other metal oxides such as Fe_3O_4, Co_3O_4 and CuO listed in **Table S3**. Although TMB shows the lowest affinity to CeO_2 cube (i.e. the highest in TMB K_m) among them, its highest H_2O_2 affinity (i.e. the lowest in H_2O_2 K_m) suggests that CeO_2 cube can be the best candidate as peroxidase mimetics among the listed metal oxides.

The interplay between H_2O_2 and CeO_2 surface was then divided into two steps for further investigation: (1) the adsorption of H_2O_2 at CeO_2 surface and (2) subsequent H_2O_2 activation by the surface Ce. Different adsorption configurations of H_2O_2 were obtained among CeO_2 surfaces in our calculation **(Figure S6)** with E_{ad} −0.68 eV for (111), −1.00 eV for (110) and −1.83 eV for (100). The most negative E_{ad} of H_2O_2 obtained on (100) surface can be attributed to the sharing of one H_2O_2 oxygen by two structural Ce atoms. Since surface peroxide species give a Raman signal at 870 cm^{-1}, *in-situ* Raman spectroscopy was carried out to monitor the activation of adsorbed H_2O_2 at CeO_2 surface (i.e. step (2)). As shown in **Figure S7**, this signal almost disappears after 16 mins for cube, while around 70% of this signal remains for octahedron after 30 mins of reaction. Linear sweep voltammetry (LSV) in **Figure S8** also confirms that the cube can provide higher current at any given voltage (> 1.75 V) among CeO_2 shapes due to surface electron-rich Ce species.

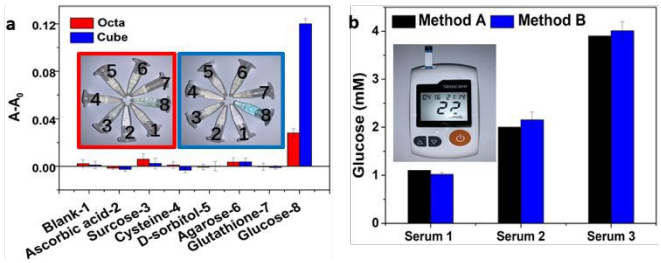

Figure 4. (a) Selectivity test of different solutions using CeO_2 octahedron (left, red highlighted) and CeO_2 cube (right, blue highlighted) as peroxidase mimetics. A and A_0 are corresponding absorbance and the absorbance of blank contrast at 652 nm. (b) Comparison of the obtained glucose level in serum samples by commercial glucose assay kit (see picture inside) (method A, Scheme 1a) and using CeO_2 cube as peroxidase mimetics (method B, Scheme 1b). Note that all error bars in this figure show the standard deviations of three replicates.

Accordingly, the O–O bond of the adsorbed H_2O_2 can be easily activated and reduced by the electron-rich Ce atom on (100) surface but not for its counterpart on (111) surface with a lower electron density. Since CeO_2 nanozyme without shape control preferentially exposes (111) surface, this may explain why limited enhancements in Ce reactivity (< 200%) were often obtained in literature even after surface modifications.[5–11]

The detection limit of H_2O_2/glucose and the corresponding linear range were further evaluated over CeO_2 octahedron and cube in **Figure S9 and Table S4** (same weight of catalyst was used). Note that the cube with one-third of $[Ce]_{surface}$ (cf. octahedron) **(Table S1)** can provide not only lower H_2O_2/glucose detection limit (more than four times) but also a wider linear range (more than five times). CeO_2 cube also outperforms other metal oxides in literature by providing lower detection limit and wider linear range **(Table S5)**. Selectivity test carried out in **Figure 4a** further demonstrates that CeO_2 cube can provide very high glucose selectivity in the consecutive enzyme reactions as peroxidase mimetics. We then examined the feasibility of replacing natural peroxidase enzyme by the CeO_2 cube in the enzymatic assay **(Scheme 1)** according to the obtained glucose level in serum samples. The testing results of commercial human serum, horse serum and fetal bovine serum, namely serum 1, serum 2 and serum 3, were summarized in **Figure 4b** and **Table S6**. A very close glucose level with acceptable relative standard deviation (RSD) can be observed for all three serum samples using a commercial glucose assay kit (method A) and CeO_2 cube as peroxidase mimetics (method B). A nearly 100% recovery can be achieved for serum samples by these two methods **(Table S6)**, indicating that the replacing of natural peroxidase enzyme by CeO_2 cube is technically feasible.

To summarize, we have unravelled the origin of pristine CeO_2 as peroxidase mimetics and demonstrated that the atomic arrangement of surface Ce and its chemical state are both critically affecting mimicking activity. The CeO_2(100) surface can efficiently facilitate H_2O_2 adsorption and subsequent activation, providing comparable H_2O_2/glucose sensitivity as natural peroxidase used in a glucose assay kit. Most importantly, we showed that the factor of the surface area only matters when surface Ce can activate the adsorbed H_2O_2. This study thus highlights the importance of surface understanding of even a pristine material can be more critical than the continuous development of its fancy derivatives without a clear guidance.

View Article Online DOI: 10.1039/D0CC03515

We thank the Hong Kong Research Grants Council (CityU 21301719), National Natural Science Foundation of China (21902138), City University of Hong Kong (projects 9667181 and 9048147).

Conflicts of interest

There are no conflicts to declare.

Notes and references

1 L. Gao, J. Zhuang, L. Nie, J. Zhang, Y. Zhang, N. Gu, T. Wang, J. Feng, D. Yang, S. Perrett, X. Yan, Nat. *Nanotechnol*. 2007, **2**, 577–583.
2 H. Wang, K. Wan, X. Shi, *Adv. Mater*. 2019, **31,** 1805368.
3 D. Jiang, D. Ni, Z. T. Rosenkrans, P. Huang, X. Yan, W. Cai, *Chem. Soc. Rev.* 2019, **48**, 3683–3704.
4 Y. Huang, J. Ren, X. Qu, *Chem. Rev.* 2019, **119,** 4357–4412.
5 E. G. Heckert, A. S. Karakoti, S, Seal, W. T. Self, *Biomaterials* 2008, **29**, 2705–2709.
6 A. A. Vernekar, T. Das, G. Mugesh, Angew. *Chem. Int. Ed.* 2016, **55**, 1412–1416.
7 Z. Tian, J. Li, Z. Zhang, W. Gao, X. Zhou, Y. Qu, *Biomaterials* 2015, **59**, 116–124.
8 T. Yao, Z. Tian, Y. Zhang, Y. Qu, *ACS Appl. Mater. Interfaces* 2019, **11,** 195–201.
9 Z. Tian, T. Yao, C. Qu, S. Zhang, X. Li, Y. Qu, *Nano Lett.* 2019, **19,** 8270–8277.
10 C. Xu, X. Qu, *NPG Asia Mater.* 2014, **6**, e90.
11 G. Wang, J. Zhang, X. He, Z. Zhang, Y. Zhao, *Chin. J. Chem.* 2017, **35**, 791–800.
12 A. Trovarelli, J. Llorca, *ACS Catal.* 2017, **7**, 4716−4735.
13 Y. Ma, W. Gao, Z. Zhang, S. Zhang, Z. Tian, Y. Liu, J. C. Ho, Y. Qu, *Surf. Sci. Rep.* 2018, **73**, 1−36.
14 M. J. Manto, P. Xie, C. Wang, *ACS Catal.* 2017, **7**, 1931−1938.
15 Y. Kosto, A. Zanut, S. Franchi, Y. Yakovlev, I. Khalakhan, V. Matolín, K. C. Prince, G. Valenti, F. Paolucci, N. Tsuda, *Appl. Surf. Sci.* 2019, **488**, 351–359.
16 Y.-K. Peng, S. C. E. Tsang, *Nano Today* 2018, **18**, 15−34.
17 T. Naganuma, *Nano Res*. 2017, **10**, 199–217.
18 V. Baldim, B. Bedioui, N. Mignet, I. Margaill, J.-F. Berret, *Nanoscale* 2018, **10**, 6971–6980.
19 Y. Yang, Z. Mao, W. Huang, L. Liu, J. Li, Q. Wu, *Sci. Rep*. 2016, **6**, 35344.
20 Z. Wu, M. Li, D. R. Mullins, S. H. Overbury, *ACS Catal.* 2012, **2,** 2224−2234.
21 Z. Wu, A. K. P. Mann, M. Li, S. H. Overbury, *J. Phys. Chem. C* 2015, **119**, 7340−7350.
22 C. Yang, X. Yu, S. Heißler, A. Nefedov, S. Colussi, J. Llorca, A. Trovarelli, Y. Wang, C. Wöll, *Angew. Chem. Int. Ed.* 2017, **56**, 375–379.
23 A. Zheng, S.-B. Liu, F. Deng, *Chem. Rev*. 2017, **117**, 12475−12531.
24 W. P. Rothwell, W. Shen, J. H. Lunsford, *J. Am. Chem. Soc.* 1984, **106**, 2452–2453.
25 Y.-K. Peng, L. Ye, J. Qu, L. Zhang, Y. Fu, I. F. Teixeira, I. J. McPherson, H. He, S. C. E. Tsang, *J. Am. Chem. Soc.* 2016, **138**, 2225–2234.
26 Y.-K. Peng, Y. Hu, H.-L. Chou, Y. Fu, I. F. Teixeira, H. He, S. C. E. Tsang, *Nat. Commun.* 2017, **8**, 675.
27 Z. Tan, G. Li, H.-L. Chou, Y. Li, X. Yi, A. H. Mahadi, A. Zheng, S. C. E. Tsang, Y.-K. Peng, *ACS Catal.* 2020, **10**, 4003−4011.
28 B. Goris, S. Turner, S. Bals, G. V. Tendeloo, *ACS Nano* 2014, **8**, 10878−10884.

Table of Contents Entry

View Article Online
DOI: 10.1039/D0CC02351E

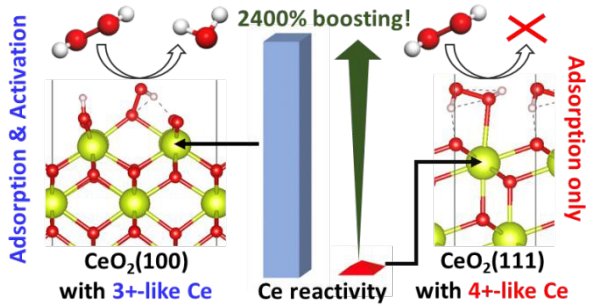

2400% increase in CeO_2 peroxidase-like activity can be easily achieved on the (100) surface due to the promoted H_2O_2 adsorption/activation.